Check for updates

AGU ADVANCING EARTH AND SPACE SCIENCES

Geophysical Research Letters®

RESEARCH LETTER
10.1029/2023GL106492

Reduced Deep Convection and Bottom Water Formation Due To Antarctic Meltwater in a Multi-Model Ensemble

Jia-Jia Chen[1,2], Neil C. Swart[3], Rebecca Beadling[4], Xuhua Cheng[1], Tore Hattermann[5], André Jüling[6], Qian Li[7], John Marshall[7,8], Torge Martin[9], Morven Muilwijk[5], Andrew G. Pauling[10], Ariaan Purich[11], Inga J. Smith[10], and Max Thomas[10]

[1]College of Oceanography, Hohai University, Nanjing, China, [2]University of Victoria, Victoria, BC, Canada, [3]Canadian Centre for Climate Modelling and Analysis, Environment and Climate Change Canada, Victoria, BC, Canada, [4]Earth and Environmental Science Department, Temple University, Philadelphia, PA, USA, [5]Norwegian Polar Institute, Fram Centre, Tromsø, Norway, [6]Royal Netherlands Meteorological Institute (KNMI), De Bilt, The Netherlands, [7]Department of Earth, Atmospheric, and Planetary Sciences, Massachusetts Institute of Technology, Cambridge, MA, USA, [8]NASA Goddard Institute for Space Studies, New York, NY, USA, [9]GEOMAR Helmholtz Centre for Ocean Research Kiel, Kiel, Germany, [10]Department of Physics, University of Otago, Dunedin, New Zealand, [11]School of Earth, Atmosphere and Environment, ARC Special Research Initiative for Securing Antarctica's Environmental Future, Monash University, Melbourne, Australia

Key Points:

- Antarctic meltwater substantially reduces the strength of simulated Southern Ocean deep convection in climate models
- The additional meltwater induces Antarctic Bottom Water warming and contraction, with dense water classes converting to lighter ones
- Differences in the magnitude of these responses between models can be partly attributed to their different base states

Supporting Information:

Supporting Information may be found in the online version of this article.

Correspondence to:

J.-J. Chen,
jiajiachen@hhu.edu.cn

Citation:

Chen, J.-J., Swart, N. C., Beadling, R., Cheng, X., Hattermann, T., Jüling, A., et al. (2023). Reduced deep convection and bottom water formation due to Antarctic meltwater in a multi-model ensemble. *Geophysical Research Letters*, *50*, e2023GL106492. https://doi.org/10.1029/2023GL106492

Received 20 SEP 2023
Accepted 4 DEC 2023

Author Contributions:

Conceptualization: Jia-Jia Chen, Neil C. Swart, Rebecca Beadling, Tore Hattermann, Qian Li, John Marshall, Torge Martin, Morven Muilwijk, Ariaan Purich, Inga J. Smith, Max Thomas
Data curation: Jia-Jia Chen, Neil C. Swart, Rebecca Beadling, Tore Hattermann, André Jüling, Qian Li, John Marshall, Torge Martin, Morven Muilwijk, Ariaan Purich, Inga J. Smith, Max Thomas

© 2023. The Authors.
This is an open access article under the terms of the Creative Commons Attribution-NonCommercial-NoDerivs License, which permits use and distribution in any medium, provided the original work is properly cited, the use is non-commercial and no modifications or adaptations are made.

Abstract The additional water from the Antarctic ice sheet and ice shelves due to climate-induced melt can impact ocean circulation and global climate. However, the major processes driving melt are not adequately represented in Coupled Model Intercomparison Project phase 6 (CMIP6) models. Here, we analyze a novel multi-model ensemble of CMIP6 models with consistent meltwater addition to examine the robustness of the modeled response to meltwater, which has not been possible in previous single-model studies. Antarctic meltwater addition induces a substantial weakening of open-ocean deep convection. Additionally, Antarctic Bottom Water warms, its volume contracts, and the sea surface cools. However, the magnitude of the reduction varies greatly across models, with differing anomalies correlated with their respective mean-state climatology, indicating the state-dependency of the climate response to meltwater. A better representation of the Southern Ocean mean state is necessary for narrowing the inter-model spread of response to Antarctic meltwater.

Plain Language Summary The melting of the Antarctic ice sheet and ice shelves can have significant impacts on ocean circulation and thermal structure, but current climate models do not fully capture these effects. In this study, we analyze seven climate models to understand how they respond to the addition of meltwater from Antarctica. We find that the presence of Antarctic meltwater leads to a significant weakening of deep convection in the open ocean. The meltwater also causes Antarctic Bottom Water to warm and its volume to decrease, while the sea surface cools and sea ice expands. However, the magnitude of the response to meltwater varies across models, suggesting that the mean-state conditions of the Southern Ocean play a role. A better representation of the mean state and the inclusion of Antarctic meltwater in climate models will help reduce uncertainties and improve our understanding of the impact of Antarctic meltwater on climate.

1. Introduction

Recent observations show that the Antarctic Ice Sheet (AIS) (Forsberg et al., 2017; IMBIE, 2018; Rignot et al., 2019) and ice shelves (Adusumilli et al., 2020; Paolo et al., 2015; Scheuchl et al., 2016) are currently losing mass, which models suggest is likely to accelerate in the coming years under high emission forcing (Deconto et al., 2021; Edwards et al., 2021; Seroussi et al., 2020). The resulting meltwater discharge into the ocean influences regional and global climate (Bronselaer et al., 2018; Dong et al., 2022; Fyke et al., 2018; Purich & England, 2023; Rye et al., 2020), and has the potential to feedback onto the rate of basal ice shelf melting (Bronselaer et al., 2018; Flexas et al., 2022; Golledge et al., 2019), although this feedback is uncertain (Beadling et al., 2022; Moorman et al., 2020). However, the time-evolving interactions between the AIS, ice shelves, and the ocean are not included in Coupled Model Intercomparison Project phases 5 and 6 models (CMIP5 and CMIP6; Taylor et al., 2012; Eyring et al., 2016; Siahaan et al., 2022). These models employ specified ice sheets, where excess water from the ice/snow layer over Antarctica is rerouted to the ocean as runoff when snow depth exceeds a certain threshold. In cases where ice shelf cavities are present, the melt rates do not evolve in time (Mathiot et al., 2017). The absence of ice sheet processes and ocean–ice interactions in coupled climate models excludes

19448007, 2023, 24, Downloaded from https://agupubs.onlinelibrary.wiley.com/doi/10.1029/2023GL106492 by Massachusetts Institute Of Technology, Wiley Online Library on [20/12/2023]. See the Terms and Conditions (https://onlinelibrary.wiley.com/terms-and-conditions) on Wiley Online Library for rules of use; OA articles are governed by the applicable Creative Commons License

Formal analysis: Jia-Jia Chen, Neil C. Swart, Rebecca Beadling, Xuhua Cheng, Tore Hattermann, André Jüling, Qian Li, John Marshall, Torge Martin, Morven Muilwijk, Andrew G. Pauling, Ariaan Purich, Inga J. Smith, Max Thomas
Funding acquisition: Xuhua Cheng, Tore Hattermann, Qian Li, John Marshall, Morven Muilwijk, Andrew G. Pauling, Ariaan Purich, Inga J. Smith, Max Thomas
Investigation: Jia-Jia Chen, Neil C. Swart, Rebecca Beadling, Xuhua Cheng, Tore Hattermann, André Jüling, Qian Li, John Marshall, Torge Martin, Morven Muilwijk, Andrew G. Pauling, Ariaan Purich, Inga J. Smith, Max Thomas
Methodology: Jia-Jia Chen, Neil C. Swart, Rebecca Beadling, Tore Hattermann, André Jüling, Qian Li, John Marshall, Torge Martin, Morven Muilwijk, Andrew G. Pauling, Ariaan Purich, Inga J. Smith, Max Thomas
Project Administration: Jia-Jia Chen, Neil C. Swart, Torge Martin, Ariaan Purich
Resources: Jia-Jia Chen, Neil C. Swart, Rebecca Beadling, Xuhua Cheng, Tore Hattermann, André Jüling, Qian Li, John Marshall, Torge Martin, Morven Muilwijk, Ariaan Purich, Inga J. Smith, Max Thomas
Software: Jia-Jia Chen, Neil C. Swart, Rebecca Beadling, Tore Hattermann, André Jüling, Qian Li, John Marshall, Torge Martin, Morven Muilwijk, Andrew G. Pauling, Ariaan Purich, Inga J. Smith, Max Thomas
Supervision: Jia-Jia Chen, Neil C. Swart
Validation: Jia-Jia Chen, Neil C. Swart, Rebecca Beadling, Xuhua Cheng, Tore Hattermann, André Jüling, Qian Li, John Marshall, Torge Martin, Morven Muilwijk, Andrew G. Pauling, Ariaan Purich, Inga J. Smith, Max Thomas
Visualization: Jia-Jia Chen
Writing – original draft: Jia-Jia Chen, Neil C. Swart
Writing – review & editing: Jia-Jia Chen, Neil C. Swart, Rebecca Beadling, Xuhua Cheng, Tore Hattermann, André Jüling, Qian Li, John Marshall, Torge Martin, Morven Muilwijk, Andrew G. Pauling, Ariaan Purich, Inga J. Smith, Max Thomas

potential feedbacks from meltwater discharge on regional and global climate, representing an unaccounted-for uncertainty in historical simulations and future projections (Swart et al., 2023).

The formation and recirculation of Antarctic Bottom Water (AABW) plays a crucial role in regulating the global climate by redistributing heat and carbon between the surface and deep ocean. In the real ocean, AABW is primarily formed by the sinking of dense waters on the Antarctic continental shelves (Orsi et al., 1999) with occasional contributions from open-ocean deep convection (Cheon & Gordon, 2019; Killworth, 1983). However, in most CMIP5 and CMIP6 models, AABW is formed by open-ocean deep convection (deep convection hereafter) with a large inter-model spread in the location and area of deep convection (Heuzé, 2021; Heuzé et al., 2013; Mohrmann et al., 2021). Simulated bottom water properties and transport are influenced by deep convection (Heuzé, 2021), which could be impacted by climate change. CMIP5 results suggest that Southern Ocean (SO) surface freshening caused by an enhanced hydrological cycle in a warming climate leads to a reduction in deep convection (De Lavergne et al., 2014). Additional surface freshening enhances the stratification by making surface waters less dense and thus the water column less prone to deep convection. Idealized model experiments also show that Antarctic meltwater forcing reduces convective depth (Fogwill et al., 2015) and suppresses the production of AABW (Lago & England, 2019; Li et al., 2023; Tesdal et al., 2023).

It remains unclear how the different representation of deep convection across models would affect the response of the SO climate to Antarctic meltwater. Inconsistent Antarctic meltwater forcing, and differing model configurations used in previous studies makes it challenging to quantify the uncertainty associated with the climate effects of Antarctic meltwater (Swart et al., 2023). For example, some studies suggest that simulated Antarctic sea-ice trends are highly sensitive to small amounts of Antarctic meltwater (10–250 Gt yr^{-1}) (Bintanja et al., 2013, 2015), while others show less sensitivity to significantly larger amounts of Antarctic meltwater (950–4,000 Gt yr^{-1}) (Pauling et al., 2016, 2017; Swart & Fyfe, 2013). A consistent experimental design applied across a wide range of climate models can help us discern robust, and model-dependent uncertainties to the meltwater forcing.

In this study, we present the first results from the new Southern Ocean Freshwater Input from Antarctica (SOFIA; Swart et al., 2023). We investigate the impacts of Antarctic meltwater on deep convection and relevant climate variables in seven different climate models following a consistent experiment protocol. We also evaluate the influence of the mean-state representation of deep convection on the modeled responses. By assessing the consistency and differences of the modeled response, this study highlights the need to understand and incorporate the effects of meltwater in future climate projections and the importance of refining and improving the representation of the Southern Ocean in climate models.

2. Methods

2.1. Models and Experimental Design

This study makes use of recent output from a novel multi-model ensemble of a coordinated Antarctic meltwater experiment, designed by the Southern Ocean Freshwater Input from Antarctica (SOFIA; Swart et al., 2023). We investigate the SOFIA Tier-1 *antwater* experiment, which imposes a temporally uniform additional freshwater flux of 0.1 Sv (1 Sv = 3.154×10^4 Gt yr^{-1}) at the ocean surface in the grid cells adjacent to the Antarctic coast, while all other forcing is taken from the CMIP6 pre-industrial control experiment (*piControl*; Eyring et al., 2016). While the observed freshwater volume associated with Antarctic ice sheet and shelves melt over 2010s is 0.017 ± 0.006 Sv (509 ± 186 Gt yr^{-1}) (Slater et al., 2021), primarily through basal melting and iceberg calving, the experiment utilizes a relatively strong but plausible freshwater forcing that may be achieved by mid-21st century under a high emission scenario (Golledge et al., 2019). Such a coordinated experimental design allows us to quantify the model similarities and differences in the climate response to Antarctic ice sheet melt among different models. Additional details about the configurations and experimental protocol can be found in Swart et al. (2023).

The simulations were run for at least 100 years, and data from seven models are currently available: ACCESS-ESM1-5 (Ziehn et al., 2020), GFDL-ESM4 (Dunne et al., 2020), GFDL-CM4 (Held et al., 2019), HadGEM3-GC31-LL (Kuhlbrodt et al., 2018), CanESM5 (Swart et al., 2019), GISS-E2-1-G (Kelley et al., 2020), and NorESM2-MM (Seland et al., 2020). These models all participated in CMIP6 and use the same configuration as in CMIP6 for the SOFIA experiment. The *piControl* run is taken from the CMIP6 output on the Earth System Grid Federation (ESGF) archive, except for GISS-E2-1-G, where the *piControl* outputs were provided directly

along with SOFIA simulations. We only use the first ensemble member for each model and analyze the first 500 years for *piControl* and the concurrent first 100 years of *antwater* to examine the response to meltwater input.

2.2. Model Output Analysis

The monthly-mean mixed layer depth (MLD) we use is the CMIP6 output variable *mlotst* (Griffies et al., 2016) defined with a density threshold of 0.125 kg m^{-3}. Despite the modeled MLD computed in this way often being deeper than observed (Heuzé, 2015, 2021), its relative change presumably provides a reasonable measure for our purpose of process investigation. The deep convection area is defined as the total surface area south of 55°S with MLD exceeding 2,000 m (De Lavergne et al., 2014). To measure the SO deep convection strength, we compute the deep-mixed volume (DMV) south of 55°S by multiplying the grid cell area by its MLD, and summing for cells with MLD exceeding 2,000 m (Brodeau & Koenigk, 2016; Heuzé, 2021). The ventilated volume of each depth range is calculated in the same way, but with 100-m MLD increments, for example, the volume at 100 m is the volume with MLD between 100 and 200 m. While we compare the *antwater* outputs with parallel 100-year *piControl* data, we use 500-year *piControl* data to assess the variability beyond the selected 100 years. To maintain equal sampling, we divide the 500-year *piControl* time series into five non-overlapping 100-year chunks (periods), each representing an ensemble realization. Then, we calculate the statistic of interest for each chunk and average the results over five chunks for the entire 500-year period. These statistical methods are justified based on the large-variability and different climatological states possible in the SO across the suite of models given SO deep-convection.

2.3. Observation-Based Reference Data

Observed temperature and salinity data from the World Ocean Atlas (WOA18; Boyer et al., 2018) are used to estimate the climatological mean state of water mass properties in the SO. The *piControl* simulations represent a quasi-equilibrium climate state under pre-industrial forcing, while the WOA18 (1955–2017) climatology provides the historical state accounting for a warming ocean, therefore the two data sets are not directly comparable. However, WOA18 can be used as a reference to contextualize our simulation and analysis results, and to better understand the potential impact of Antarctic meltwater on the SO.

To assess the simulation of deep convection in the SO, we utilize the monthly-mean MLD obtained from the European Centre for Medium-Range Weather Forecasts (ECMWF) OCEAN5 ocean analysis-reanalysis (ORAS5: Ocean Reanalysis System 5) spanning from 1958 to 2022, with a horizontal resolution of approximately 0.25° × 0.25° (Copernicus Climate Change Service). This MLD metric is defined as the depth where the average sea water density exceeds the surface density plus 0.03 kg m^{-3}. The use of lower density criteria in reanalysis may result in shallower MLD compared to the criteria of 0.125 kg m^{-3} used in CMIP6 (Heuzé, 2015). While the ORAS5 data set provides an estimate of the historical evolution of the ocean representing a different period to the *piControl* simulations, it remains a useful reference for our analysis.

3. Results

3.1. Meltwater-Induced Reduction in Deep Convection

To examine the spatial variability of deep convection in the SO given its reported differences in location and strength across models (Heuzé, 2021; Heuzé et al., 2013), we first analyzed the maximum MLD in each model's *piControl* simulation. Deep convection, indicated by black contours of 2,000 m MLD (Figure 1), primarily occurs in the Weddell Sea and Ross Sea, varying in areal extents across models (from 0.38 × 10^5 km^2 in CanESM5 to 28.93 × 10^5 km^2 in ACCESS-ESM1-5; Table S1 in Supporting Information S1). Our focus is on how the models respond to the meltwater perturbation, which allows us to concentrate on the physics related to external freshwater forcing. This approach also permits us to assess the role of the model's mean state, but the underlying causes of climatological differences are beyond the scope of this paper.

In response to meltwater forcing, the maximum MLD decreases in all models. The reduction can be up to 4,000 m (blue shading in Figure 1). These changes suggest a near-complete cessation of deep convection in those regions except ACCESS-ESM1-5. In most deep convection regions in ACCESS-ESM1-5, the maximum MLD still reaches the bottom in *antwater*. Notably, models ACCESS-ESM1-5 and HadGEM3-GC31-LL show a positive

19448007, 2023, 24, Downloaded from https://agupubs.onlinelibrary.wiley.com/doi/10.1029/2023GL106492 by Massachusetts Institute Of Technology, Wiley Online Library on [20/12/2023]. See the Terms and Conditions (https://onlinelibrary.wiley.com/terms-and-conditions) on Wiley Online Library for rules of use; OA articles are governed by the applicable Creative Commons License

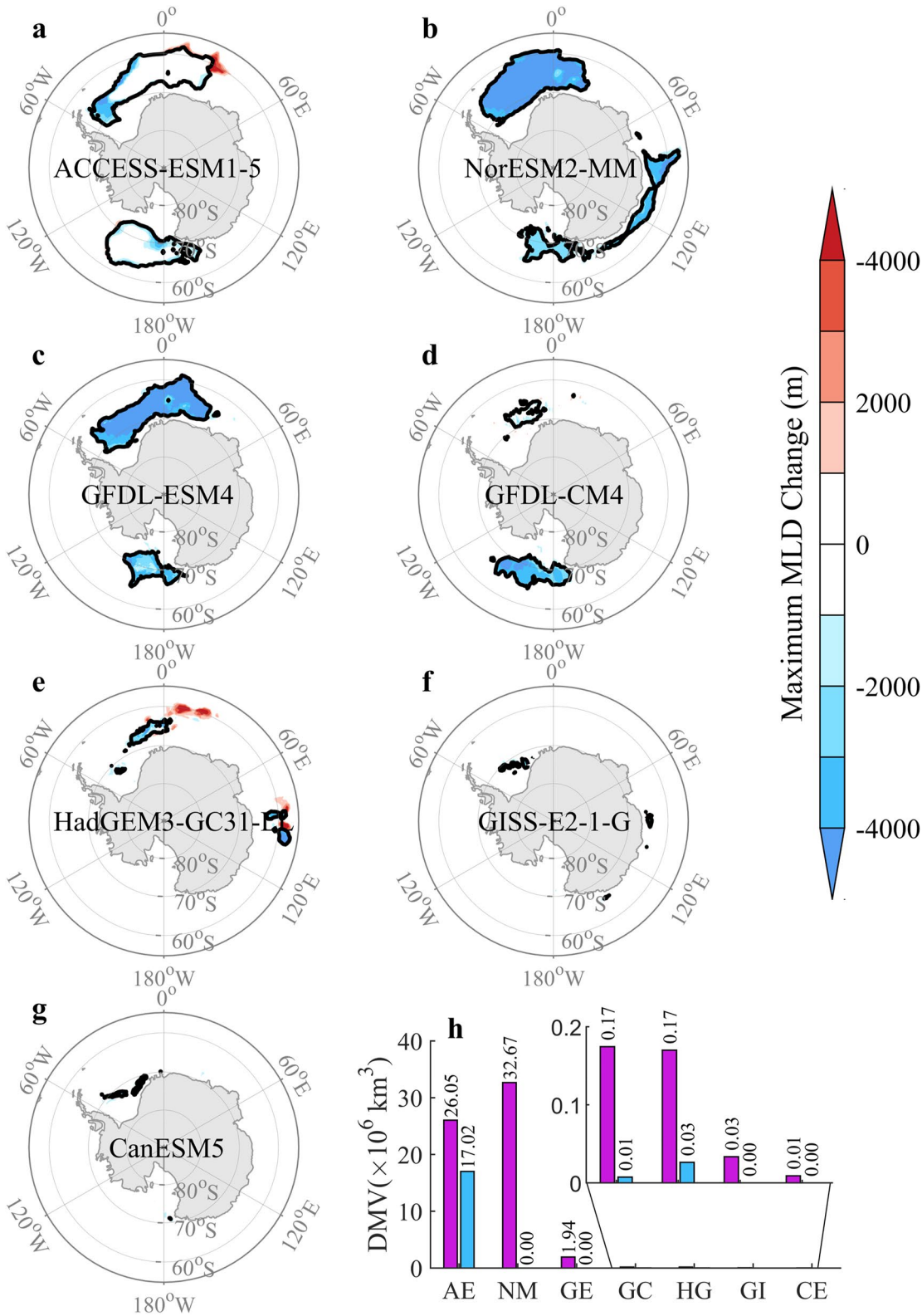

Figure 1. Response of Southern Ocean deep convection to meltwater. (a–g) Maximum mixed layer depth (MLD) change (shading; *antwater* - *picontrol*) south of 55°S across various models, each labeled in the center of its respective subplots. The black contour is 2,000 m of maximum MLD in *piControl*, delineating the location of deep convection. (h) Climatological annual deep mixed volume (DMV) south of 55°S for *piControl* (purple) and *antwater* (blue), with values at the top of each bar corresponding to models: ACCESS-ESM1-5 (AE), NorESM2-MM (NM), GFDL-ESM4 (GE), GFDL-CM4 (GC), HadGEM3-GC31-LL (HG), GISS-E2-1-G (GI), and CanESM5 (CE).

19448007, 2023, 24, Downloaded from https://agupubs.onlinelibrary.wiley.com/doi/10.1029/2023GL106492 by Massachusetts Institute Of Technology, Wiley Online Library on [20/12/2023]. See the Terms and Conditions (https://onlinelibrary.wiley.com/terms-and-conditions) on Wiley Online Library for rules of use; OA articles are governed by the applicable Creative Commons License

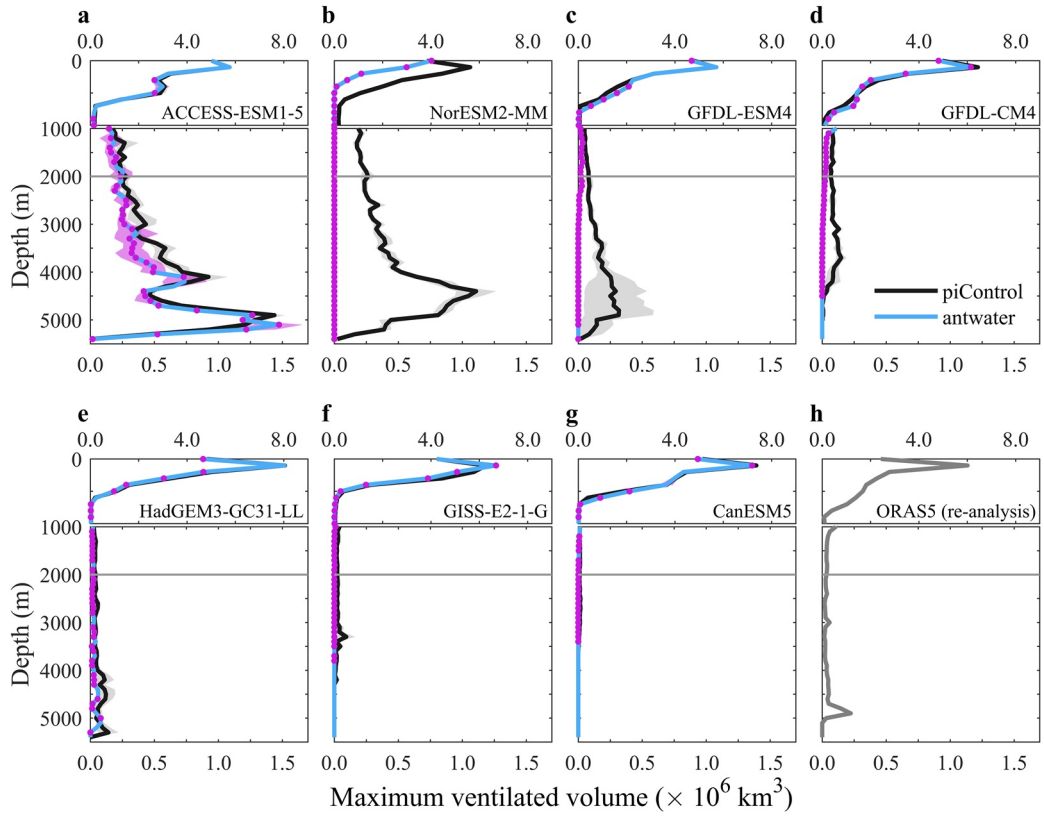

Figure 2. Vertical profiles of Southern Ocean convection: (a–g) Maximum ventilated volume in *piControl* (average, black; gray shading refers to one standard deviation) and in *antwater* (average, blue; purple dot where significant determined through a bootstrapping test, please refer to SI for details) across various models, each labeled within its respective subplots. For each column, the upper and lower panels represent the above 1,000 and 1,000–5,500 m depth ranges, respectively. Note that the horizontal and vertical scales changes between the upper (0–9 × 10^6 km^3) and lower parts (0–1.75 × 10^6 km^3) of each panel. (h) Maximum ventilated volume from ORAS5 re-analysis data over 1958–2022.

anomaly patch at the edge of the *piControl* deep convection region, possibly indicating a location shift of the deep convection. These findings indicate that meltwater forcing has a significant impact on the MLD and deep convection in the SO, but the response varies across models.

The maximum ventilated volume at each depth range provides a more detailed picture of how convective mixing responds to the meltwater forcing (Figure 2). All models exhibit a consistent vertical distribution in *piControl*, with relatively large volumes below 2,000 m and above 1,000 m, although the magnitudes differ among models. In *antwater*, all models, except ACCESS-ESM1-5, experience an extreme reduction in ventilated volume to nearly zero below 2,000 m, while the shallow (<500 m) mixed volume decreases by less than ∼30% or even increases at certain depths (Figure S1 in Supporting Information S1). This implies that the impact of the meltwater on the convective mixing varies with depth and is greater on deep ocean convection than on shallow mixing. Both ACCESS-ESM1-5 and NorESM2-MM have a significantly larger ventilated volume below 2,000 m in *piControl* compared to the other models and the re-analysis and display a larger change in response to meltwater. Averaged annual deep mixed volumes (DMV; Figure 1h) also exhibit substantial reduction to nearly zero in all models except ACCESS-ESM1-5, which still maintains strong deep convection. The magnitude of deep convection response has a high correlation with its mean-state value ($r^2 = 0.79$, $p < 0.01$). The additional freshwater further reduces the already low frequency of deep convection (Figure S2 in Supporting Information S1), with some models showing no occurrence for 100 consecutive years (Table S1 in Supporting Information S1). To account for potential sampling biases introduced by the meltwater simulations only performed for 100 years, and the long timescale variability of the SO, we conduct a bootstrapping test by randomly resampling 1,000 times from the *piControl* data (please refer to SI for details). The gray shading in Figure 2 represents the range of one standard deviation of the maximum ventilated volume obtained from the resampled data. The statistically

19448007, 2023, 24, Downloaded from https://agupubs.onlinelibrary.wiley.com/doi/10.1029/2023GL106492 by Massachusetts Institute Of Technology, Wiley Online Library on [20/12/2023]. See the Terms and Conditions (https://onlinelibrary.wiley.com/terms-and-conditions) on Wiley Online Library for rules of use; OA articles are governed by the applicable Creative Commons License

19448007, 2023, 24, Downloaded from https://agupubs.onlinelibrary.wiley.com/doi/10.1029/2023GL106492 by Massachusetts Institute Of Technology, Wiley Online Library on [20/12/2023]. See the Terms and Conditions (https://onlinelibrary.wiley.com/terms-and-conditions) on Wiley Online Library for rules of use; OA articles are governed by the applicable Creative Commons License

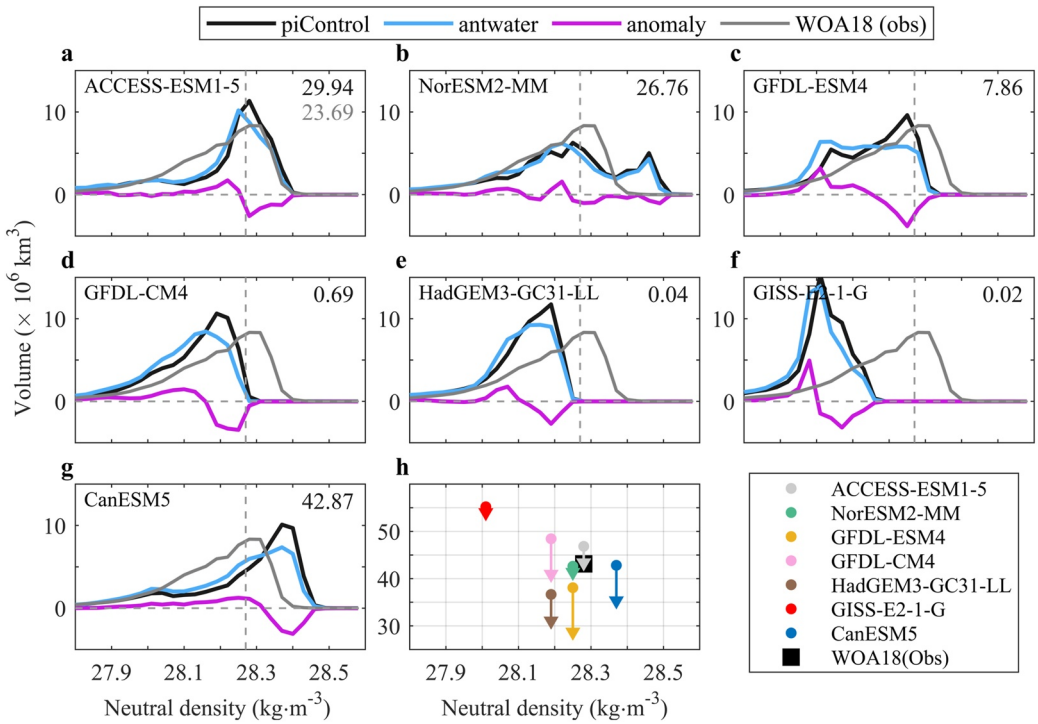

Figure 3. Volumetric distribution of water masses plotted by density south of 60°S from *piControl* (black), *antwater* (light blue), and the difference (purple). The observed distribution (light gray) from WOA18 is averaged from 1955 to 2017. The black number in the top-right corner of each panel is the simulated volume ($\times 10^6$ km^3) with density greater than 28.27 kg m^{-3}, indicated by a vertical gray line. The gray number in panel (a) represents the observed volume from WOA18. (h) Integrated volumes within a 0.18 kg m^{-3} range near the volume peak of each model are depicted as dots in *piControl*, arrows in *antwater*, and a black square for WOA18.

significant reduction in deep convection (Figure S3 in Supporting Information S1; purple dots in Figure 2) indicates that the result is not an artifact of the sampling uncertainty.

3.2. Reduced Antarctic Bottom Water Volume

Open-ocean deep convection is the main production mechanism of AABW in most CMIP6 models and reduced deep convection could have a large influence on simulated local and global climate by reducing the AABW formation rate (De Lavergne et al., 2014; Lago & England, 2019; Purich & England, 2023). However, it is not yet clear how the response of AABW formation and volume to Antarctic meltwater differs or is similar among different climate models.

AABW is typically defined by a neutral density greater than 28.27 kg m^{-3} (Orsi et al., 1999). We analyze the AABW properties south of 60°S, consistent with the established AABW cell definition (Lago & England, 2019), emphasizing the AABW signal. The AABW volume derived from WOA18 is about 23.69 × 10^6 km^3, roughly 32% of the total water volume in this region. The models display a wide variation in the distribution pattern of water masses density south of 60°S (Figure 3). This variability across models results in a wide range of AABW volume, spanning from 0.02 × 10^6 km^3 (GISS-E2-1-G) to 43.52 × 10^6 km^3 (CanESM5) across models (black curves and numbers in Figure 3) based on the observed-climatology criteria of 28.27 kg m^{-3}. The AABW volume change in response to meltwater has a high correlation with the AABW volume in the models' climatological mean state ($r^2 = 0.93$, $p < 0.01$; Figure S4c in Supporting Information S1). The AABW volume change ($\sigma = 3.50$) across models shows less variability than the climatological mean AABW volume ($\sigma = 17.74$) in *piControl*.

Despite large biases in the water mass properties, all models show a consistent contraction in the densest waters south of 60°S (purple curves in Figure 3), corresponding to a warming of the deep ocean (Figure 4). To better assess the volume changes of bottom water due to meltwater influence, a critical neutral density is determined at the position of maximum volume for each model. The integrated volume near this neutral density decreases across

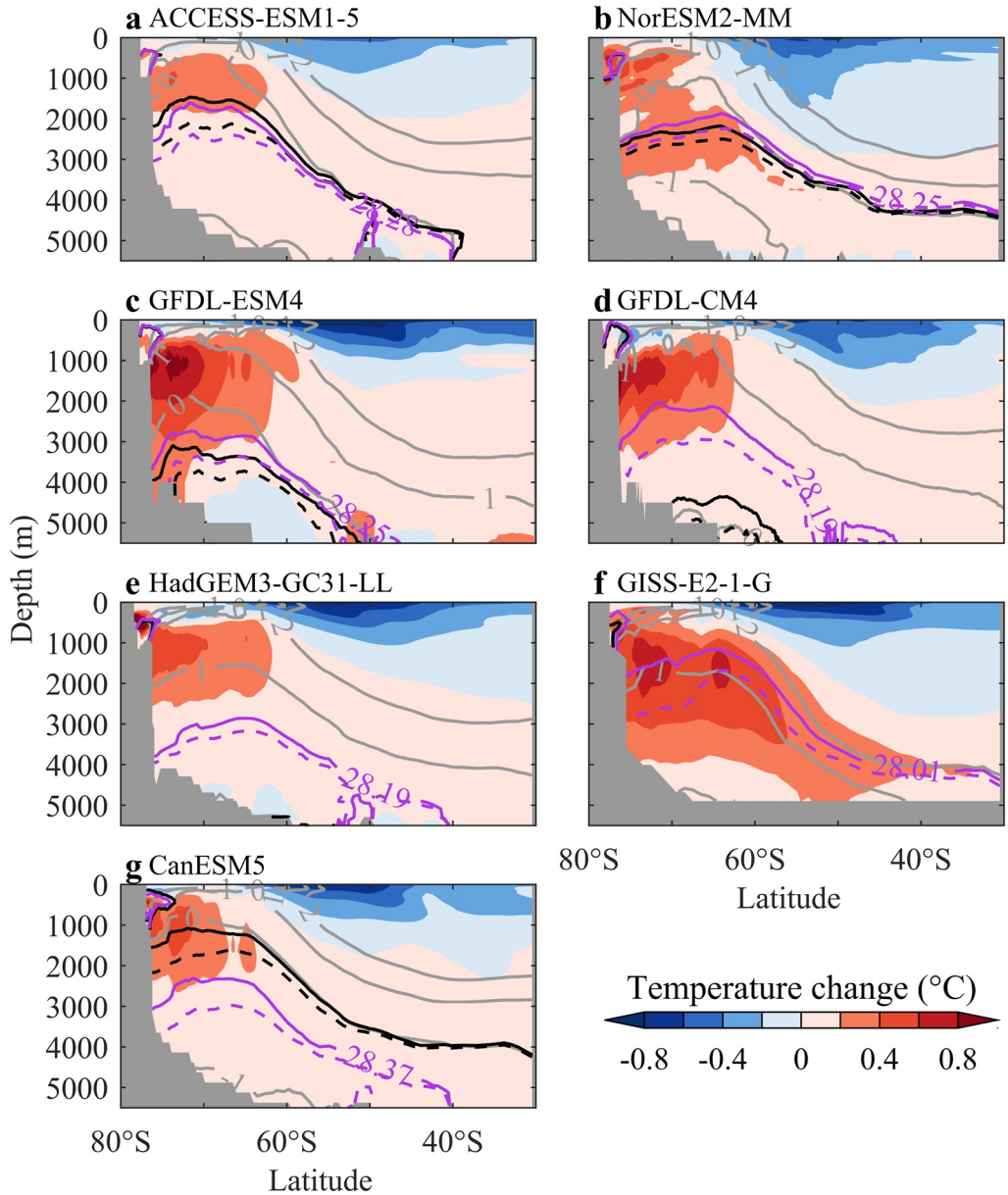

Figure 4. Zonal mean potential temperature change (°C; shading; *antwater - picontrol*). Solid gray contours show the climatological temperature in *piControl*. Black lines represent the 28.27 kg m^{-3} neutral density in *piControl* (solid line) and *antwater* (dashed line). Purple lines denote neutral density corresponding to the volume peak (see black line in Figure 3) observed in *piControl*.

all models (Figure 3h), with this neutral density being represented by the purple contours in Figure 4. The volume of the lighter water masses (e.g., around 28 kg m^{-3}) increases due to the upper ocean freshening. The consistent pattern of surface cooling and deep ocean warming at high latitudes might result from common processes and responses to the meltwater forcing shared among models, such as decreased deep convection discussed earlier. However, no significant linear relationship is found between the magnitudes of AABW contraction and the change or base state of deep convection (Figure S5 in Supporting Information S1). This suggests that other processes may also affect AABW. All models also show a reduced AABW overturning circulation and increased sea ice extent (Figure S5 in Supporting Information S1), possibly contributing to surface cooling and deep ocean warming. However, without further analysis of the associated processes, we cannot attribute the changes to any specific process.

19448007, 2023, 24, Downloaded from https://agupubs.onlinelibrary.wiley.com/doi/10.1029/2023GL106492 by Massachusetts Institute Of Technology, Wiley Online Library on [20/12/2023]. See the Terms and Conditions (https://onlinelibrary.wiley.com/terms-and-conditions) on Wiley Online Library for rules of use; OA articles are governed by the applicable Creative Commons License

4. Discussion and Conclusions

This study analyzed the novel multi-model experiment *antwater*, which is specified as a part of the coordinated experimental designs proposed by SOFIA (Swart et al., 2023). Our analysis of seven climate models consistently shows a significant decrease in deep convection (Figures 1 and 2), contraction of Antarctic Bottom Water (AABW) (Figure 3) and warming of the deep ocean (Figure 4) in response to meltwater forcing. In *piControl*, all seven models exhibit deep convection in the Southern Ocean (SO), primarily in the Weddell and Ross Sea. Adding meltwater at the surface increases water column stratification at high latitudes, where density is dominated by salinity (De Lavergne et al., 2014; Purich & England, 2023), leading to reduction in deep convection. This finding is consistent with previous single-model studies (Fogwill et al., 2015; Lago & England, 2019; Li et al., 2023).

Observations suggest that Dense Shelf Water (DSW) overflow is the primary contributor to AABW (Orsi et al., 1999, 2002), and DSW formation is sensitive to the meltwater (Hattermann et al., 2021; Silvano et al., 2018). However, most CMIP6 models simulate AABW formation via deep convection due to the limitations of their coarse resolution (Heuzé, 2021; Mohrmann et al., 2021; Purich & England, 2021). Changes in deep convection may impact deep-ocean properties and circulation (Heuzé, 2021; Zanowski et al., 2015). The reduced deep convection hinders the sinking of cold surface water, contributing to deep-ocean warming and AABW volume contraction, consistent with previous studies on Antarctic meltwater effects (Li et al., 2023; Mackie et al., 2020; Park & Latif, 2019). However, we found no strong correlation between deep convection and deep-ocean warming across seven models (Figure S4 in Supporting Information S1), suggesting other factors like enhanced stratification, may also contribute to deep warming and surface cooling by limiting upward vertical mixing of subsurface heat (Chen et al., 2022). Furthermore, the meltwater-induced poleward shift of warm, saline Circumpolar Deep Water and the weakening of the lower cell of the overturning circulation (Figure S4 in Supporting Information S1) could also be associated with deep-ocean warming (Li et al., 2023; Moorman et al., 2020; Purich & England, 2021). These mechanisms may have already influenced SO climate, evident in observed AABW warming and contraction (Aoki et al., 2015; Purkey & Johnson, 2010, 2013; Shimada et al., 2022), overturning slowdown (Gunn et al., 2023; Zhou et al., 2023), as well as surface cooling or delayed warming south of the ACC (Armour et al., 2016; Haumann et al., 2020). It is noted that our results are based on an idealized experiment with meltwater input of greater magnitude than historically observed mass loss from Antarctic grounded and floating ice shelves (Slater et al., 2021), and thus cannot be directly applied to interpret observed changes in the SO. Nevertheless, our study suggests that inclusion of changing Antarctic meltwater in coupled climate models is important due to the far-reaching climate responses in the SO.

In addition to the robust responses, it is important to consider the variability among models. The magnitudes of changes in both deep convection and AABW volume varies strongly across models and are correlated with their respective mean state in *piControl* ($r^2 = 0.79$ and $r^2 = 0.93$, respectively; Figure S4 in Supporting Information S1) This indicates that the models' base state strongly influence deep convection and AABW volume anomalies. Differences in the ocean temperature changes (Figure 4) also exist among models, but no robust correlation is found between the anomalies and mean state magnitudes. Future research could benefit from including a larger model ensemble in intermodel comparisons to further evaluate the robustness of the results presented here.

We acknowledge that meltwater from Antarctica's ice shelves enters the ocean over a certain depth range instead of at the surface and also may be spatially distributed farther offshore by icebergs rather than only along the coast, both of which may have implications for the responses presented here. Unlike in reality, where the majority of mass loss occurs near Amundsen Sea (Davison et al., 2023; IMBIE, 2018), this study assumes a uniform distribution of meltwater surrounding the Antarctic coast. However, previous studies have not found substantial sensitivity to the different location of meltwater input (Park & Latif, 2019; Swart & Fyfe, 2013), which may be advected around the continent within about ten years (Dawson et al., 2023). Incorporating a more realistic representation of meltwater would enhance our understanding of its influence. These uncertainties are addressed in SOFIA Tier-2 and Tier-3 experiments (Swart et al., 2023), and could be examined once the model output becomes available. It is noteworthy that the intermodel differences in mean state are always larger than those in the response, particularly for deep convection volume and deep ocean temperature. This underscores the necessity for coupled climate models to accurately capture the SO's mean state, including a more realistic simulation of dense water formation, thereby reducing model uncertainty and improving models' performance in projecting future changes.

19448007, 2023, 24, Downloaded from https://agupubs.onlinelibrary.wiley.com/doi/10.1029/2023GL106492 by Massachusetts Institute Of Technology, Wiley Online Library on [20/12/2023]. See the Terms and Conditions (https://onlinelibrary.wiley.com/terms-and-conditions) on Wiley Online Library for rules of use; OA articles are governed by the applicable Creative Commons License

Data Availability Statement

The authors acknowledge the use of various data sets that significantly contributed to this research. The data of the freshwater experiments are available in Swart et al. (2023), the CMIP6 piControl experiments Eyring et al. (2016). The WOA18 data (potential temperature and salinity) are available in Boyer et al. (2018) and ORAS5 re-analysis data (mixed layer depth) are from Copernicus Climate Change Service (2021).

Acknowledgments
JJC and XHC acknowledge the support from the Natural Science Foundation of China (nos. 41876002). MM and TH were supported by funding from the European Union's Horizon 2020 research and innovation programme under grant agreement No 101003826 via project CRiceS. QL and JM were supported by the NASA MAP program 19-MAP19-0011 and the MIT-GISS cooperative agreement. The model simulations and analysis were conducted on the NASA High-End Computing (HEC) Program through the NASA Center for Climate Simulation (NCCS) at Goddard Space Flight Center. MT, AGP, and IJS were supported by the Deep South National Science Challenge (MBIE C01X1412) and the Antarctic Science Platform (University of Otago subcontract 19424 from VUW's ASP Project 4 contract with Antarctica New Zealand through MBIE SSIF Programmes Investment ANTA1801), and acknowledge use of high performance computing facilities, consulting support, and training services from New Zealand eScience Infrastructure (NeSI: funded by collaborator institutions and through MBIE's Research Infrastructure programme). AP was supported by the Australian Research Council Special Research Initiative for Securing Antarctica's Environmental Future (SR200100005).

References

Adusumilli, S., Fricker, H. A., Medley, B., Padman, L., & Siegfried, M. R. (2020). Interannual variations in meltwater input to the southern ocean from Antarctic ice shelves. *Nature Geoscience*, *13*(9), 616–620. https://doi.org/10.1038/s41561-020-0616-z

Aoki, S., Mizuta, G., Sasaki, H., Sasai, Y., Rintoul, S. R., & Bindoff, N. L. (2015). Atlantic–Pacific asymmetry of subsurface temperature change and frontal response of the Antarctic circumpolar current for the recent three decades. *Journal of Oceanography*, *71*(5), 623–636. https://doi.org/10.1007/s10872-015-0284-6

Armour, K. C., Marshall, J., Scott, J. R., Donohoe, A., & Newsom, E. R. (2016). Southern Ocean warming delayed by circumpolar upwelling and equatorward transport. *Nature Geoscience*, *9*(7), 549–554. https://doi.org/10.1038/ngeo2731

Beadling, R. L., Krasting, J. P., Griffies, S. M., Hurlin, W. J., Bronselaer, B., Russell, J. L., et al. (2022). Importance of the Antarctic slope current in the southern ocean response to ice sheet melt and wind stress change. *Journal of Geophysical Research: Oceans*, *127*(5), e2021JC017608. https://doi.org/10.1029/2021jc017608

Bintanja, R., Van Oldenborgh, G. J., Drijfhout, S. S., Wouters, B., & Katsman, C. A. (2013). Important role for ocean warming and increased ice-shelf melt in Antarctic sea-ice expansion. *Nature Geoscience*, *6*(5), 376–379. https://doi.org/10.1038/ngeo1767

Bintanja, R., Van Oldenborgh, G. J., & Katsman, C. A. (2015). The effect of increased fresh water from Antarctic ice shelves on future trends in Antarctic sea ice. *Annals of Glaciology*, *56*(69), 120–126. https://doi.org/10.3189/2015AoG69A001

Boyer, T. P., García, H. E., Locarnini, R. A., Zweng, M. M., Mishonov, A. V., Reagan, J. R., et al. (2018). World ocean atlas [Dataset]. National Environmental Satellite, Data, and Information Service. National Centers for Environmental Information (U.S.). https://repository.library.noaa.gov/view/noaa/49137

Brodeau, L., & Koenigk, T. (2016). Extinction of the northern oceanic deep convection in an ensemble of climate model simulations of the 20th and 21st centuries. *Climate Dynamics*, *46*(9–10), 2863–2882. https://doi.org/10.1007/s00382-015-2736-5

Bronselaer, B., Winton, M., Griffies, S., Hurlin, W., Rodgers, K., Sergienko, O., et al. (2018). Change in future climate due to Antarctic meltwater. *Nature*, *564*(7734), 53–58. https://doi.org/10.1038/s41586-018-0712-z

Chen, J.-J., Swart, N. C., & Cheng, X. (2022). Processes controlling the Southern Ocean temperature change. *Journal of Climate*, *35*(23), 7739–7749. https://doi.org/10.1175/jcli-d-22-0111.1

Cheon, W. G., & Gordon, A. L. (2019). Open-ocean polynyas and deep convection in the Southern Ocean. *Scientific Reports*, *9*(1), 1–9. https://doi.org/10.1038/s41598-019-43466-2

Copernicus Climate Change Service, Climate Data Store. (2021). ORAS5 global ocean reanalysis monthly data from 1958 to present [Dataset]. Copernicus Climate Change Service (C3S) Climate Data Store (CDS). https://doi.org/10.24381/cds.67e8eeb7

Davison, B. J., Hogg, A. E., Rigby, R., Veldhuijsen, S., van Wessem, J. M., van den Broeke, M. R., et al. (2023). Sea level rise from West Antarctic mass loss significantly modified by large snowfall anomalies. *Nature Communications*, *14*(1), 1479. https://doi.org/10.1038/s41467-023-36990-3

Dawson, H. R. S., Morrison, A. K., England, M. H., & Tamsitt, V. (2023). Pathways and timescales of connectivity around the Antarctic continental shelf. *Journal of Geophysical Research: Oceans*, *128*(2), 1–25. https://doi.org/10.1029/2022JC018962

Deconto, R. M., Pollard, D., Alley, R. B., Velicogna, I., Gasson, E., Gomez, N., et al. (2021). The Paris climate agreement and future sea-level rise from Antarctica. *Nature*, *593*(7857), 83–89. https://doi.org/10.1038/s41586-021-03427-0

De Lavergne, C., Palter, J. B., Galbraith, E. D., Bernardello, R., & Marinov, I. (2014). Cessation of deep convection in the open Southern Ocean under anthropogenic climate change. *Nature Climate Change*, *4*(4), 278–282. https://doi.org/10.1038/nclimate2132

Dong, Y., Pauling, A. G., Sadai, S., & Armour, K. C. (2022). Antarctic ice-sheet meltwater reduces transient warming and climate sensitivity through the sea-surface temperature pattern effect. *Geophysical Research Letters*, *49*(24), 1–11. https://doi.org/10.1029/2022GL101249

Dunne, J. P., Horowitz, L. W., Adcroft, A. J., Ginoux, P., Held, I. M., John, J. G., et al. (2020). The GFDL Earth system model version 4.1 (GFDL - ESM 4.1): Overall coupled model description and simulation characteristics journal of advances in modeling Earth systems. *Journal of Advances in Modeling Earth Systems*, *12*(11), 1–56. https://doi.org/10.1029/2019MS002015

Edwards, T. L., Nowicki, S., Marzeion, B., Hock, R., Goelzer, H., Seroussi, H., et al. (2021). Projected land ice contributions to twenty-first-century sea level rise. *Nature*, *593*(7857), 74–82. https://doi.org/10.1038/s41586-021-03302-y

Eyring, V., Bony, S., Meehl, G. A., Senior, C. A., Stevens, B., Stouffer, R. J., & Taylor, K. E. (2016). Overview of the coupled model intercomparison project phase 6 (CMIP6) experimental design and organization [Dataset]. Geoscientific Model Development, *9*(5), 1937–1958. https://doi.org/10.5194/gmd-9-1937-2016

Flexas, M. M., Thompson, A. F., Schodlok, M. P., Zhang, H., & Speer, K. (2022). Antarctic Peninsula warming triggers enhanced basal melt rates throughout West Antarctica. *Science Advances*, *8*(32), 1–12. https://doi.org/10.1126/sciadv.abj9134

Fogwill, C. J., Phipps, S. J., Turney, C. S. M., & Golledge, N. R. (2015). Sensitivity of the Southern Ocean to enhanced regional Antarctic ice sheet meltwater input. *Earth's Future*, *3*(10), 317–329. https://doi.org/10.1002/2015EF000306

Forsberg, R., Sørensen, L., & Simonsen, S. (2017). Greenland and Antarctica ice sheet mass changes and effects on global sea level. *Surveys in Geophysics*, *38*(1), 89–104. https://doi.org/10.1007/s10712-016-9398-7

Fyke, J., Sergienko, O., Löfverström, M., Price, S., & Lenaerts, J. T. M. (2018). An overview of interactions and feedbacks between ice sheets and the Earth system. *Reviews of Geophysics*, *56*(2), 361–408. https://doi.org/10.1029/2018RG000600

Golledge, N. R., Keller, E. D., Gomez, N., Naughten, K. A., Bernales, J., Trusel, L. D., & Edwards, T. L. (2019). Global environmental consequences of twenty-first-century ice-sheet melt. *Nature*, *566*(7742), 65–72. https://doi.org/10.1038/s41586-019-0889-9

Griffies, S. M., Danabasoglu, G., Durack, P. J., Adcroft, A. J., Balaji, V., Böning, C. W., et al. (2016). OMIP contribution to CMIP6: Experimental and diagnostic protocol for the physical component of the Ocean Model Intercomparison Project. *Geoscientific Model Development*, *9*(9), 3231–3296. https://doi.org/10.5194/gmd-9-3231-2016

Gunn, K. L., Rintoul, S. R., England, M. H., & Bowen, M. M. (2023). Recent reduced abyssal overturning and ventilation in the Australian Antarctic Basin. *Nature Climate Change*, *13*(6), 537–544. https://doi.org/10.1038/s41558-023-01667-8

19448007, 2023, 24, Downloaded from https://agupubs.onlinelibrary.wiley.com/doi/10.1029/2023GL106492 by Massachusetts Institute Of Technology, Wiley Online Library on [20/12/2023]. See the Terms and Conditions (https://onlinelibrary.wiley.com/terms-and-conditions) on Wiley Online Library for rules of use; OA articles are governed by the applicable Creative Commons License

Hattermann, T., Nicholls, K. W., Hellmer, H. H., Davis, P. E. D., Janout, M. A., Østerhus, S., et al. (2021). Observed interannual changes beneath Filchner-Ronne Ice Shelf linked to large-scale atmospheric circulation. *Nature Communications*, *12*(1), 1–11. https://doi.org/10.1038/s41467-021-23131-x

Haumann, F. A., Gruber, N., & Münnich, M. (2020). Sea-ice induced Southern Ocean subsurface warming and surface cooling in a warming climate. *AGU Advances*, *1*(2), e2019AV000132. https://doi.org/10.1029/2019av000132

Held, I. M., Guo, H., Adcroft, A., Dunne, J. P., Horowitz, L. W., Krasting, J., et al. (2019). Structure and performance of GFDL's CM4. 0 climate. *Model Journal of Advances in Modeling Earth Systems*, *11*(11), 3691–3727. https://doi.org/10.1029/2019MS001829

Heuzé, C. (2015). *Antarctic bottom water in CMIP5 models: Characteristics, formation, evolution* (PhD thesis). University of East Anglia. Retrieved from https://ueaeprints.uea.ac.uk/id/eprint/53396

Heuzé, C. (2021). Antarctic bottom water and north Atlantic deep water in CMIP6 models. *Ocean Science*, *17*(1), 59–90. https://doi.org/10.5194/os-17-59-2021

Heuzé, C., Heywood, K. J., Stevens, D. P., & Ridley, J. K. (2013). Southern Ocean bottom water characteristics in CMIP5 models. *Geophysical Research Letters*, *40*(7), 1409–1414. https://doi.org/10.1002/grl.50287

IMBIE, T. (2018). Mass balance of the Antarctic ice sheet from 1992 to 2017. *Nature*, *558*(7709), 219–222. https://doi.org/10.1038/s41586-018-0179-y

Kelley, M., Schmidt, G. A., Nazarenko, L. S., Bauer, S. E., Ruedy, R., Russell, G. L., et al. (2020). GISS-E2.1: Configurations and climatology. *Journal of Advances in Modeling Earth Systems*, *12*(8), e2019MS002025. https://doi.org/10.1029/2019MS002025

Killworth, P. D. (1983). Deep convection in the World Ocean. *Reviews of Geophysics and Space Physics*, *21*(1), 1–26. https://doi.org/10.1029/rg021i001p00001

Kuhlbrodt, T., Jones, C. G., Sellar, A., Storkey, D., Blockley, E., Stringer, M., et al. (2018). The low-resolution version of HadGEM3 GC3. 1: Development and evaluation for global climate. *Journal of Advances in Modeling Earth Systems*, 2865–2888. https://doi.org/10.1029/2018MS001370

Lago, V., & England, M. H. (2019). Projected slowdown of Antarctic bottom water formation in response to amplified meltwater contributions. *Journal of Climate*, *32*(19), 6319–6335. https://doi.org/10.1175/JCLI-D-18-0622.1

Li, Q., England, M. H., Hogg, A. M., Rintoul, S. R., & Morrison, A. K. (2023). Supplementary to Abyssal ocean overturning slowdown and warming driven by Antarctic meltwater. *Nature*, *615*, 841–847. https://doi.org/10.1038/s41586-023-05762-w

Mackie, S., Smith, I. J., Ridley, J. K., Stevens, D. P., & Langhorne, P. J. (2020). Climate response to increasing Antarctic iceberg and ice shelf melt. *Journal of Climate*, *33*(20), 8917–8938. https://doi.org/10.1175/JCLI-D-19-0881.1

Mathiot, P., Jenkins, A., Harris, C., & Madec, G. (2017). Explicit representation and parametrised impacts of under ice shelf seas in the z∗- coordinate ocean model NEMO 3.6. *Geoscientific Model Development*, *10*(7), 2849–2874. https://doi.org/10.5194/gmd-10-2849-2017

Mohrmann, M., Heuzé, C., & Swart, S. (2021). Southern Ocean polynyas in CMIP6 models. *The Cryosphere*, *15*(9), 4281–4313. https://doi.org/10.5194/tc-15-4281-2021

Moorman, R., Morrison, A. K., & Hogg, A. M. C. (2020). Thermal responses to antarctic ice shelf melt in an eddy-rich global ocean–sea ice model. *Journal of Climate*, *33*(15), 6599–6620. https://doi.org/10.1175/JCLI-D-19-0846.1

Orsi, A. H., Johnson, G. C., & Bullister, J. L. (1999). Circulation, mixing, and production of Antarctic bottom water. *Progress in Oceanography*, *43*(1), 55–109. https://doi.org/10.1016/S0079-6611(99)00004-X

Orsi, A. H., Smethie, W. M., & Bullister, J. L. (2002). On the total input of Antarctic waters to the deep ocean: A preliminary estimate from chlorofluorocarbon measurements. *Journal of Geophysical Research*, *107*(C8), 31-1–31-14. https://doi.org/10.1029/2001jc000976

Paolo, F., Fricker, H., & Padman, L. (2015). Volume loss from Antarctic ice shelves is accelerating. *Science*, *348*(6232), 327–331. https://doi.org/10.1126/science.aaa0940

Park, M., & Latif, W. (2019). Ensemble global warming simulations with idealized Antarctic meltwater input. *Climate Dynamics*, *52*(5), 3223–3239. https://doi.org/10.1007/s00382-018-4319-8

Pauling, A. G., Bitz, C. M., Smith, I. J., & Langhorne, P. J. (2016). The response of the southern ocean and Antarctic sea ice to freshwater from ice shelves in an Earth system model. *Journal of Climate*, *29*(5), 1655–1672. https://doi.org/10.1175/JCLI-D-15-0501.1

Pauling, A. G., Smith, I. J., Langhorne, P. J., & Bitz, C. M. (2017). Time-dependent freshwater input from ice shelves: Impacts on Antarctic sea ice and the southern ocean in an Earth system model. *Geophysical Research Letters*, *44*(20), 10454–10461. https://doi.org/10.1002/2017GL075017

Purich, A., & England, M. H. (2021). Historical and future projected warming of antarctic shelf bottom water in CMIP6 models. *Geophysical Research Letters*, *48*(10), 1–15. https://doi.org/10.1029/2021GL092752

Purich, A., & England, M. H. (2023). Projected impacts of Antarctic meltwater anomalies over the twenty-first century. *Journal of Climate*, *36*(8), 2703–2719. https://doi.org/10.1175/JCLI-D-22-0457.1

Purkey, S. G., & Johnson, G. C. (2010). Warming of global abyssal and deep Southern Ocean waters between the 1990s and 2000s: Contributions to global heat and sea level rise budgets. *Journal of Climate*, *23*(23), 6336–6351. https://doi.org/10.1175/2010JCLI3682.1

Purkey, S. G., & Johnson, G. C. (2013). Antarctic bottom water warming and freshening: Contributions to sea level rise, ocean freshwater budgets, and global heat gain. *Journal of Climate*, *26*(16), 6105–6122. https://doi.org/10.1175/JCLI-D-12-00834.1

Rignot, E., Mouginot, J., Scheuchl, B., Van Den Broeke, M., Van Wessem, M. J., & Morlighem, M. (2019). Four decades of Antarctic ice sheet mass balance from 1979–2017. *Proceedings of the National Academy of Sciences of the United States of America*, *116*(4), 1095–1103. https://doi.org/10.1073/pnas.1812883116

Rye, C. D., Marshall, J., Kelley, M., Russell, G., Nazarenko, L., Kostov, Y., et al. (2020). Antarctic glacial melt as a driver of recent southern ocean climate trends. *Geophysical Research Letters*, *47*(11), e2019GL086892. https://doi.org/10.1029/2019gl086892

Scheuchl, B., Mouginot, J., Rignot, E., Morlighem, M., & Khazendar, A. (2016). Grounding line retreat of Pope, Smith, and Kohler Glaciers, west Antarctica, measured with Sentinel-1a radar interferometry data. *Geophysical Research Letters*, *43*(16), 8572–8579. https://doi.org/10.1002/2016GL069287

Seland, Ø., Bentsen, M., Olivié, D., Toniazzo, T., Gjermundsen, A., Graff, L. S., et al. (2020). Overview of the Norwegian Earth System Model (NorESM2) and key climate response of CMIP6 DECK, historical, and scenario simulations. *Geoscientific Model Development*, *13*(12), 6165–6200. https://doi.org/10.5194/gmd-13-6165-2020

Seroussi, H., Nowicki, S., Payne, A. J., Goelzer, H., Lipscomb, W. H., Abe-Ouchi, A., et al. (2020). ISMIP6 Antarctica: A multi-model ensemble of the Antarctic ice sheet evolution over the 21st century. *The Cryosphere*, *14*(9), 3033–3070. https://doi.org/10.5194/tc-14-3033-2020

Shimada, K., Kitade, Y., Aoki, S., Mizobata, K., Cheng, L., Takahashi, K. T., et al. (2022). Shoaling of abyssal ventilation in the Eastern Indian Sector of the Southern Ocean. *Communications Earth and Environment*, *3*(1), 1–9. https://doi.org/10.1038/s43247-022-00445-2

Siahaan, A., Smith, R. S., Holland, P. R., Jenkins, A., Gregory, J. M., Lee, V., et al. (2022). The Antarctic contribution to 21st-century sea-level rise predicted by the UK Earth System Model with an interactive ice sheet. *The Cryosphere*, *16*(10), 4053–4086. https://doi.org/10.5194/tc-16-4053-2022

19448007, 2023, 24, Downloaded from https://agupubs.onlinelibrary.wiley.com/doi/10.1029/2023GL106492 by Massachusetts Institute Of Technology, Wiley Online Library on [20/12/2023]. See the Terms and Conditions (https://onlinelibrary.wiley.com/terms-and-conditions) on Wiley Online Library for rules of use; OA articles are governed by the applicable Creative Commons License

Silvano, A., Rintoul, S. R., Peña-molino, B., Hobbs, W. R., Wijk, E. V., Aoki, S., et al. (2018). Freshening by glacial meltwater enhances melting of ice shelves and reduces formation of Antarctic Bottom Water. *Science Advances*, *4*, 1–12. https://doi.org/10.1126/sciadv.aap9467

Slater, T., Lawrence, I. R., Otosaka, I. N., Shepherd, A., Gourmelen, N., Jakob, L., et al. (2021). Review article: Earth's ice imbalance. *The Cryosphere*, *15*(1), 233–246. https://doi.org/10.5194/tc-15-233-2021

Swart, N., & Fyfe, J. (2013). The influence of recent Antarctic ice sheet retreat on simulated sea ice area trends. *Geophysical Research Letters*, *40*(16), 4328–4332. https://doi.org/10.1002/GRL.50820

Swart, N., Martin, T., Beadling, R., Chen, J.-J., England, M. H., Farneti, R., et al. (2023). The Southern Ocean freshwater input from Antarctica (SOFIA) initiative: Scientific objectives and experimental design [Dataset]. *EGUsphere*, *2023*, 1–30. https://doi.org/10.5194/egusphere-2023-198

Swart, N. C., Cole, J. N., Kharin, V. V., Lazare, M., Scinocca, J. F., Gillett, N. P., et al. (2019). The Canadian earth system model version 5 (CanESM5. 0.3). *Geoscientific Model Development*, *12*(11), 4823–4873. https://doi.org/10.5194/gmd-12-4823-2019

Taylor, K., Stouffer, R., & Meehl, G. (2012). An overview of CMIP5 and the experiment design. *Bulletin of the American Meteorological Society*, *93*(4), 485–498. https://doi.org/10.1175/BAMS-D-11-00094.1

Tesdal, J., MacGilchrist, G. A., Beadling, R. L., Griffies, S. M., Krasting, J. P., & Durack, P. J. (2023). Revisiting interior water mass responses to surface forcing changes and the subsequent effects on overturning in the Southern Ocean. *Journal of Geophysical Research: Oceans*, *128*(3), e2019GL086892. https://doi.org/10.1029/2022jc019105

Zanowski, H., Hallberg, R., & Sarmiento, J. L. (2015). Abyssal ocean warming and salinification after weddell polynyas in the GFDL CM2G coupled climate model. *Journal of Physical Oceanography*, *45*(11), 2755–2772. https://doi.org/10.1175/JPO-D-15-0109.1

Zhou, S., Meijers, A. J. S., Meredith, M. P., Abrahamsen, E. P., Holland, P. R., Silvano, A., et al. (2023). Slowdown of Antarctic Bottom Water export driven by climatic wind and sea-ice changes. *Nature Climate Change*, *13*(7), 701–709. https://doi.org/10.1038/s41558-023-01695-4

Ziehn, T., Chamberlain, M. A., Law, R. M., Lenton, A., Bodman, R. W., Dix, M., et al. (2020). The Australian Earth system model: ACCESS-ESM1.5. *Journal of Southern Hemisphere Earth Systems Science*, *70*(1), 193–214. https://doi.org/10.1071/ES19035

19448007, 2023, 24, Downloaded from https://agupubs.onlinelibrary.wiley.com/doi/10.1029/2023GL106492 by Massachusetts Institute Of Technology, Wiley Online Library on [20/12/2023]. See the Terms and Conditions (https://onlinelibrary.wiley.com/terms-and-conditions) on Wiley Online Library for rules of use; OA articles are governed by the applicable Creative Commons License